Metastability in pressure-induced structural transformations of CdSe/ZnS core/shell nanocrystals

Michael Grünwald and Katie Lutker

Department of Chemistry, University of California, Berkeley, California 94720

A. Paul Alivisatos

Department of Chemistry, University of California, Berkeley, and Materials Sciences Division, Lawrence Berkeley National Laboratories, Berkeley, California 94720

Eran Rabani

School of Chemistry, The Sackler Faculty of Exact Sciences, Tel Aviv University, Tel Aviv 69978, Israel

Phillip L. Geissler

Department of Chemistry, University of California, Berkeley, and Lawrence Berkeley National Laboratories, Berkeley, California 94720

arXiv:1201.3162v1 [cond-mat.mtrl-sci] 16 Jan 2012

Abstract

The kinetics and thermodynamics of structural transformations under pressure depend strongly on particle size due to the influence of surface free energy [1–4]. By suitable design of surface structure [5], composition [6] and passivation [2] it is possible, in principle, to prepare nanocrystals in structures inaccessible to bulk materials [7]. However, few realizations of such extreme size-dependent behavior exist [8]. Here we show with molecular dynamics computer simulation that in a model of CdSe/ZnS core/shell nanocrystals the core high pressure structure can be made metastable under ambient conditions by tuning the thickness of the shell. In nanocrystals with thick shells, we furthermore observe a wurtzite to NiAs transformation, which does not occur in the pure bulk materials. These phenomena are linked to a fundamental change in the atomistic transformation mechanism from heterogenous nucleation at the surface to homogenous nucleation in the crystal core. Our results suggest a new route towards expanding the range of available nanoscale materials.

At thermodynamic equilibrium, matter adopts the form that minimizes its total free energy [9]. Close to first-order phase transitions, however, metastability of the competing phases is often observed; liquid water can be cooled many degrees below its freezing point, magnets can withstand oppositely oriented magnetic fields, and diamonds do not transform to graphite at ambient conditions. How far one can push a system out of its equilibrium phase depends on the microscopic transformation mechanism that determines the height of the free energy barrier separating the competing phases.

Exploiting the metastability of different solid phases is a possible route to creating materials with new properties. However, many crystal structures form only when high pressure is applied and are unstable under ambient conditions in the bulk. In nanocrystals, on the other hand, phase diagrams and microscopic transformation mechanisms can depend strongly on particles' size and shape [5, 10]. The wurtzite to rocksalt transformation in CdSe nanocrystals, for example, shows an increasing thermodynamic transition pressure and a decreasing activation enthalpy with decreasing particles size [2, 11, 12]. While it is in principle possible to extend the metastability of high-pressure structures to ambient conditions by engineering the surface properties of nanoparticles, significant insight into the underlying microscopic transformation dynamics is required.

A particularly interesting surface modification is realized in core/shell nanocrystals [13], where the core material is epitaxially overgrown with a material of identical crystal structure [14–16]. While the optical qualities of these hetero-materials are well-studied [17], little is known about their structural properties [18]. In modern synthesis methods, materials with a lattice mismatch of up to 11% can be combined to form a pristine core/shell interface [17]. The resulting lattices of both core and shell experience a strong strain that depends sensitively on particle size and has the potential of introducing dramatic changes to the nanoparticle's structural and kinetic behavior under pressure.

In this Letter, we report the simulation of spherical wurtzite CdSe nanocrystals of 3 nm diameter (510 atoms), that have been epitaxially passivated with ZnS shells of thicknesses up to 2.1 nm (5 monolayers). The largest of these core/shell crystals consists of 6918 atoms. The particles are modeled with empirical pair potentials designed to reproduce a number of properties of the bulk materials [19, 20]. In our simulations, a single crystal is immersed in a pressure bath of ideal gas particles [21, 22] at a temperature of 300 K and the pressure is increased in steps of 0.2 GPa every 10 ps. These pressurization rates are many orders of

magnitude larger than in experiments using diamond anvil cells but are comparable to recent shock-wave experiments on CdSe nanocrystals [23]. When a pressure of 20 GPa is reached after 1 ns, the pressure is released again at the same rate. After reaching ambient pressures, the crystals are simulated for another 1.2 ns. We monitor the evolution of the crystal structure by calculating atom-coordination numbers based on the radial pair distribution functions of core and shell atoms.

The effect of the ZnS shell on the structure of the CdSe core is dramatic. In Figure 1B we plot the density of the wurtzite core of crystals with different shell sizes as a function of external pressure. The density of the core increases significantly with increasing shell thickness. For a 2 nm shell, this compression effect is equivalent to an additional external pressure of 6 GPa, as illustrated in Figure 1C. This pressure is much higher than the bulk coexistence pressure of 2.4 GPa of our CdSe model, and high enough to cause spontaneous transformation in bare CdSe crystals. Similarly high pressures were found at the core/shell interface in experiments of CdS/ZnS nanocrystals [24]. One might therefore expect the transformation in core/shell crystals to happen at lower pressures compared to bare CdSe nanocrystals. Quite to the contrary, the upstroke transformation pressure of the core increases strongly with increasing shell size, as illustrated in Figure 2. While pure CdSe nanocrystals transform at around 6 GPa, transformation pressures of up to 18 GPa are observed for crystals with thick shells.

Our simulations suggest that the increase in upstroke transformation pressure with particle size is caused by an increase in thermodynamic transition pressure and a concurrent removal of favorable surface nucleation sites. We estimated the phase diagram of the nanoparticles by calculating the pressures at which crystals in different phases have equal enthalpy (see Figure 2). In particular, we consider three combinations of core/shell crystal structures: wurtzite/wurtzite, rocksalt/wurtzite, and rocksalt/rocksalt. A shell thickness of 0.5 nm, corresponding to a single monolayer of ZnS, is enough to raise the thermodynamic transition pressure by 2 GPa. With increasing shell size, the phase boundary of the all-rocksalt phase approaches the bulk thermodynamic transition pressure of our ZnS model. At larger shell sizes (3–4 monolayers), the rocksalt/wurtzite phase, featuring distinct crystal structures in the core and shell, appears as a stable intermediate between the homogenous phases. The thermodynamic transformation pressure from the all-wurtzite to the heterogenous phase is fairly insensitive to shell thickness, indicating that a large-shell regime has been reached.

The appearance of the rocksalt/wurtzite phase is accompanied by a fundamental change of nucleation mechanism. Computer simulations of pure CdSe nanocrystals have shown that crystals with low energy surface facets always transform via nucleation events on the surface.[4, 12] While we observe similar surface nucleation in core/shell crystals with shell thicknesses up to 3 monolayers, for crystals with thick shells nucleation happens in the core, as illustrated in Figure 3. Despite the nearly constant thermodynamic transition pressure in this size-regime, the observed transformation pressures still increased. This indicates that the change from heterogeneous to homogeneous nucleation results in an increase in the size of the nucleation barrier.

While a typical core transformation event lasts no longer than 10 ps, transformations of shells proceed in steps, creating only confined regions of rocksalt at a time. The hysteresis curves in Figure 3 manifest such dynamics. By 20 GPa, however, most shells have completed the transformation to rocksalt By comparison, we found that a pure 4 nm ZnS nanocrystal remained in the wurtzite structure when subjected to the same pressure protocol, indicating that the core also influences the shell. Upon release of pressure, all crystal shells undergo a back-transformation: Thick shells transform back to a mixture of wurtzite/zinc-blende, thin shells to predominantly amorphous four-coordinated structures.

Not all crystal cores, on the other hand, underwent a back-transformation. While crystal cores with thin shells ($\lesssim 1$ monolayers) and thick shells ($\gtrsim 4$ monolayers) transform back to mixtures of wurtzite and zinc-blende structures, cores in a broad range of intermediate shell sizes remain in the rocksalt structure down to zero pressure, as illustrated in Figure 4. This observation suggests a significant increase of the down-stroke kinetic barrier with increasing shell thickness. The nature of this increased barrier height is related to the interface between the rocksalt core and the re-transformed shell. During the back-transformation of the shell, bonds between core and shell atoms stay mostly intact. The re-transformed shell neatly passivates the rocksalt core and thus removes favorable nucleation sites at the core surface. The amorphization of shells thinner than 1 nm upon back-transformation is a consequence of this passivation and the mismatch between the rocksalt and wurtzite structures in the core and shell, respectively. Very thick shells, however, transform back into crystalline wurtzite/zinc-blende mixtures and induce larger stress at the core/shell interface, facilitating the back-transformation of the core. Our simulations demonstrate that rocksalt cores can persist on the nanosecond timescale; recent experiments suggest substantial metastability

even on experimental timescales [18].

Phase transitions that occur far from equilibrium do not necessarily lead to the phase with the lowest free energy. In fact, Ostwald's step rule predicts that a system will transform from a metastable phase to the phase with the smallest free energy difference. In an unexpected realization of this rule of thumb, we observed a wurtzite to NiAs (B8) transformation in a few crystals with thick shells. Figure 5A shows three snapshots of a 1.9 nm shell crystal. In the course of the transformation a grain boundary between the expected rocksalt structure and the NiAs structure builds up in the core and later propagates into the shell at higher pressures. Like rocksalt, the NiAs structure is 6-coordinated. Cations are in a rocksalt-type coordination environment, while anions are coordinated by a trigonal prism of cations (Figure 5B). The occurrence of the NiAs structure is surprising, since it has not been observed experimentally in the pure materials, neither in the bulk nor in nanocrystals. Figure 5C shows a plot of the bulk enthalpies of the core and shell materials in the wurtzite, rocksalt and NiAs structures as a function of pressure. Throughout the pressure range studied here (0–20 GPa), NiAs is never enthalpically most stable. However, it becomes metastable with respect to the wurtzite structure at pressures larger than 4.5 GPa and 16 GPa, for CdSe and ZnS, respectively. (The transformation illustrated in Figure 5C occurred at 17 GPa.) Interestingly, in a recent pressure study of ZnS/CdSe core/shell nanocrystals an unexpected Raman peak was observed after the transformation had happened [25].

In summary, we have shown that both the kinetics and thermodynamics of the wurtzite to rocksalt transformation in CdSe/ZnS core/shell crystals are strongly affected by the thickness of the shell. A strong increase in thermodynamic transition pressure with increasing shell thickness is accompanied by a substantial broadening of the hysteresis, rendering the transformed rocksalt cores metastable at ambient conditions. The up-stroke nucleation pathway changes from heterogenous nucleation on the surface to homogenous nucleation in the core. In thick-shell crystals, the greatly increased up-stroke transformation pressure can lead to nucleation of the NiAs structure, which is not observed in the two pure materials.

The unexpected occurrence of a new high-pressure NiAs structure suggests that other materials might be susceptible to a similar phenomenon. By artificially increasing the pressures at which solid-solid transformation take place, transformation routes to other, previously unobservable crystal structures might become available. Potentially, such an increase can be achieved by blocking favorable nucleation pathways through suitable surface modifications,

or by using high pressurization rates as obtained in shockwave experiments.

Methods

The interatomic pair potential for ZnS was obtained using the same procedure outlined in Ref. [20] and consists of a Lennard-Jones part and electrostatic interactions. Potential parameters are given in Table I. Standard mixing rules were used for interactions between unlike atom types. The equations of motion were integrated with the velocity Verlet algorithm [26] and a time step of 2 fs. The ideal gas barostat was parameterized as in Ref. [22].

	q(e)	σ(Å)	ϵ(K)
Zn	1.18	0.02	17998.4
S	-1.18	4.90	16.5
Cd	1.18	1.98	16.8
Se	-1.18	5.24	14.9

TABLE I. Potential parameters for ZnS and CdSe [20].

To generate core/shell nanocrystals, we place Cd, Se, Zn, and S atoms on a contiguous subset of the lattice sites that define a bulk wurtzite crystal with lattice constants $a = 4.3$ Å and $c = 7.0$ Å. A roughly spherical shape is obtained by including in this subset only lattice sites lying within a distance $r = 15\,\text{Å} + r_{\text{shell}}$ away from the center of a particular (arbitrary) unit cell. Surface energies are reduced by subsequently excluding lattice sites possessing fewer than two nearest neighbors. Atoms are positioned on the resulting subset of lattice sites as follows: (i) Cd and Se are placed on all "a" and "b" sites, respectively, within a radius of 15 Å of the center. (ii) Zn and S atoms are placed on all remaining "a" and "b" sites, respectively. (iii) In a final step designed to mimic effects of CdSe core relaxation prior to shell growth, all Cd and Se atoms bound to fewer than two Se and Cd atoms, respectively, are replaced by Zn and S atoms, respectively.

Coarse-grained atom densities were computed as

$$\bar{\rho}(\mathbf{r}) = \left(2\pi\sigma^2\right)^{-3/2} \sum_{i=1}^{N} \exp\left(\frac{(\mathbf{r}-\mathbf{r}_i)^2}{2\sigma^2}\right), \tag{1}$$

where $\mathbf{r}_i$ is the position of atom i, and N is the total number of atoms. The effective atomic width $\sigma = 2$ Å was chosen to balance smoothness and resolution of $\bar{\rho}(\mathbf{r})$. The density profile $\rho(r)$ plotted in Figure 1A was computed by averaging $\bar{\rho}(\mathbf{r})$ within thin spherical shells centered on the nanocrystal's center of mass: The core density values in Figure 1B were further averaged over distances within 8 Å of the nanocrystal's center of mass.

Points of equal enthalpy in Figure 2 were determined in NPT-Monte Carlo simulations as described in Ref. [12]. Initial configurations were extracted from the molecular dynamics trajectories in which the transformations were observed. Bulk enthalpies in Figure 5 were calculated in NPT-Monte Carlo simulations of approximately 500 periodically replicated atoms. Ewald sums were used for the calculation of electrostatic interactions [26].

Hysteresis curves in Figures 3 and 4 show the fraction of 4- and 6-coordinated atoms in the core and shell, respectively. These fractions were calculated as follows: For every configuration along a given trajectory, the radial pair distribution function $g(r)$ was calculated separately for core and shell atoms and averaged over 5 ps intervals. The first minimum of $g(r)$ was found numerically and the respective distance used as a cutoff for the calculation of the number of nearest neighbors. To minimize interfacial contributions, only core atoms within 10 Å of the center of mass were included in the calculation; likewise, shell atoms within 18 Å of the center were excluded.

[1] Tolbert, S. H. & Alivisatos, A. P. Size Dependence of a First Order Solid-Solid Phase Transition: The Wurtzite to Rock Salt Transformation in CdSe Nanocrystals. *Science* **265**, 373–376 (1994).

[2] Chen, C.-C., Herhold, A. B., Johnson, C. S. & Alivisatos, A. P. Size Dependence of Structural Metastability in Semiconductor Nanocrystals. *Science* **276**, 398 (1997).

[3] Jacobs, K., Zaziski, D., Scher, E. C., Herhold, A. B. & Alivisatos, A. P. Activation Volumes for Solid-Solid Transformations in Nanocrystals. *Science* **293**, 1803 (2001).

[4] Grünwald, M. & Dellago, C. Nucleation and growth in structural transformations of nanocrystals. *Nano Lett.* **9**, 2099–102 (2009).

[5] Grünwald, M., Rabani, E. & Dellago, C. Mechanisms of the Wurtzite to Rocksalt Transformation in CdSe Nanocrystals. *Phys. Rev. Lett.* **96**, 255701 (2006).

[6] Farvid, S. S., Dave, N., Wang, T. & Radovanovic, P. V. Dopant-Induced Manipulation of the Growth and Structural Metastability of Colloidal Indium Oxide Nanocrystals. *J. Phys. Chem. C* **113**, 15928–15933 (2009).

[7] Jacobs, K., Wickham, J. & Alivisatos, A. P. Threshold Size for Ambient Metastability of Rocksalt CdSe Nanocrystals. *J. Phys. Chem. B* **106**, 3759 (2002).

[8] Dinega, D. P. & Bawendi, M. G. A Solution-Phase Chemical Approach to a New Crystal Structure of Cobalt. *Angewandte Chemie International Edition* **38**, 1788–1791 (1999).

[9] Callen, H. B. *Thermodynamics and an Introduction to Thermostatistics* (John Wiley & Sons, New York, 1985), 2 edn.

[10] Bealing, C., Fugallo, G., Martonak, R. & Molteni, C. Constant pressure molecular dynamics simulations for ellipsoidal, cylindrical and cuboidal nano-objects based on inertia tensor information. *Phys. Chem. Chem. Phys.* **12**, 8542–8550 (2010).

[11] Tolbert, S. H. & Alivisatos, A. P. The wurtzite to rock salt structural transformation in CdSe nanocrytsals under high pressure. *J. Chem. Phys.* **102**, 4642 (1995).

[12] Grünwald, M. & Dellago, C. Transition state analysis of solid-solid transformations in nanocrystals. *J. Chem. Phys.* **131**, 164116 (2009).

[13] Spanhel, L., Haase, M., Weller, H. & Henglein, A. Photochemistry of colloidal semiconductors. 20. surface modification and stability of strong luminescing cds particles. *J. Am. Chem. Soc.*

109, 5649–5655 (1987).

[14] Hines, M. A. & Guyot-Sionnest, P. Synthesis and characterization of strongly luminescing zns-capped cdse nanocrystals. *J. Phys. Chem.* **100**, 468 (1996).

[15] Dabbousi, B. O. *et al.* (CdSe) ZnS Core-Shell Quantum Dots : Synthesis and Characterization of a Size Series of Highly Luminescent Nanocrystallites. *J. Phys. Chem. B* **101**, 9463–9475 (1997).

[16] Peng, X., Schlamp, M. C., Kadavanich, A. V. & Alivisatos, A. P. Epitaxial Growth of Highly Luminescent CdSe/CdS Core/Shell Nanocrystals with Photostability and Electronic Accessibility. *Journal of the American Chemical Society* **119**, 7019–7029 (1997).

[17] Rosenthal, S., Mcbride, J., Pennycook, S. & Feldman, L. Synthesis, surface studies, composition and structural characterization of CdSe, core/shell and biologically active nanocrystals. *Surface Science Reports* **62**, 111–157 (2007).

[18] Li, Z. *et al.* The structural transition behavior of CdSe/ZnS core/shell quantum dots under high pressure. *Physica Status Solidi (B)* **248**, 1149–1153 (2011).

[19] Rabani, E. Structure and electrostatic properties of passivated CdSe nanocrystals. *J. Chem. Phys.* **115**, 1493 (2001).

[20] Rabani, E. An interatomic pair potential for cadmium selenide. *J. Chem. Phys.* **116**, 258 (2002).

[21] Grünwald, M. & Dellago, C. Ideal gas pressure bath: a method for applying hydrostatic pressure in the computer simulation of nanoparticles. *Mol. Phys.* **104**, 3709 (2006).

[22] Grünwald, M., Geissler, P. L. & Dellago, C. An efficient transition path sampling algorithm for nanoparticles under pressure. *J. Chem. Phys.* **127**, 154718 (2007).

[23] Wittenberg, J., Merkle, M. & Alivisatos, A. P. Wurtzite to Rocksalt Phase Transformation of Cadmium Selenide Nanocrystals via Laser-Induced Shock Waves: Transition from Single to Multiple Nucleation. *Phys. Rev. Lett.* **103**, 1–4 (2009).

[24] Ithurria, S., Guyot-Sionnest, P., Mahler, B. & Dubertret, B. Mn^{2+} as a radial pressure gauge in colloidal core/shell nanocrystals. *Phys. Rev. Lett.* **99**, 265501 (2007).

[25] Fan, H. M. *et al.* High pressure photoluminescence and Raman investigations of CdSeZnS core/shell quantum dots. *Appl. Phys. Lett.* **90**, 021921 (2007).

[26] Frenkel, D. & Smit, B. *Understanding Molecular Simulation* (Academic Press, New York, 2002).

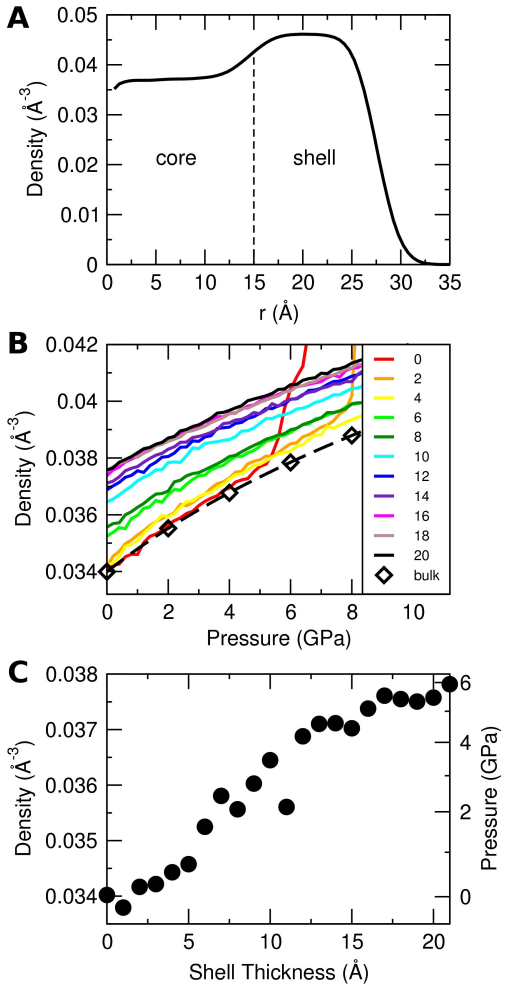


FIG. 1. **The ZnS shell compresses the CdSe core.** (**A**) Coarse-grained atom density of a 1.5 nm shell-crystal at zero pressure as a function of distance r from the center of mass. The different densities of the core and shell materials are well visible. (**B**) Density of the core as a function of pressure, for nanocrystals with different shell thickness (legend values indicate shell thickness in Å). The density of bulk CdSe, obtained from constant pressure Monte Carlo simulations, is shown for reference. The dashed line is a fit of the bulk data to the Murnaghan equation of state. Note that the sudden increase in density observed for 0 and 0.2 nm shell-crystals is a signature of the wurtzite to rocksalt transformation. (**C**) Core density at zero pressure as a function of shell thickness. The right hand ordinate shows the pressure necessary to achieve equivalent densities in bulk CdSe.

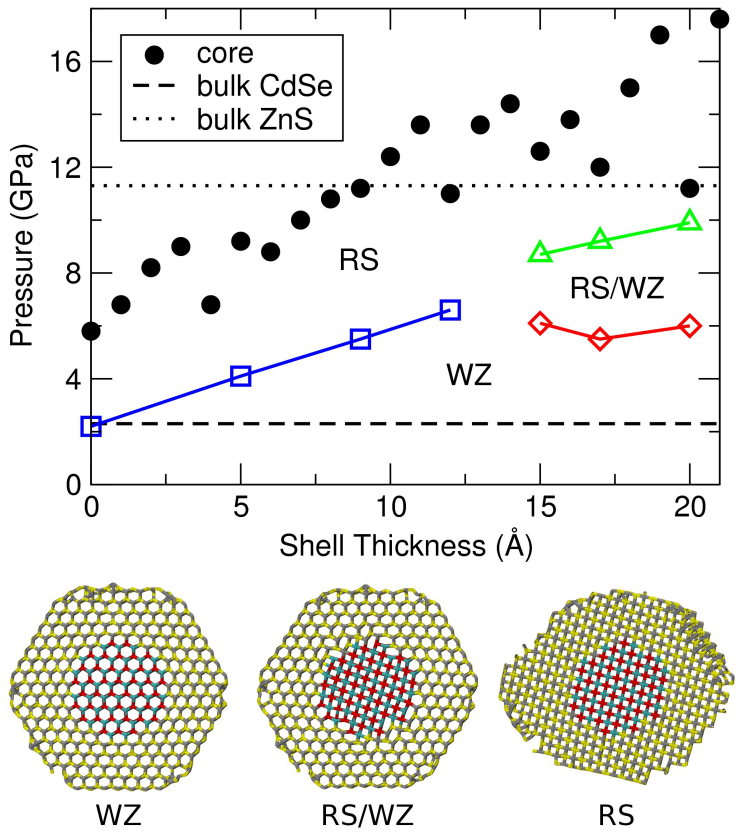


FIG. 2. **Size-dependent transformation pressure.** Core upstroke transformation pressures (solid black circles) are plotted as a function of shell thickness. At these pressures, the fraction of six-coordinated atoms exceeds 0.1 for the first time. The thermodynamic transition pressure of bulk CdSe (dashed line) and bulk ZnS (dotted line) are shown for reference. Points of equal enthalpy (blue squares and red diamonds), obtained from constant pressure Monte Carlo simulations, give an estimate of the nanocrystal phase diagram as a function of shell thickness. The three phases are illustrated below the graph as cross sections of a 2 nm shell crystal: wurtzite core and shell (WZ), a rocksalt core in a wurtzite shell (RS/WZ), and rocksalt core and shell (RS).

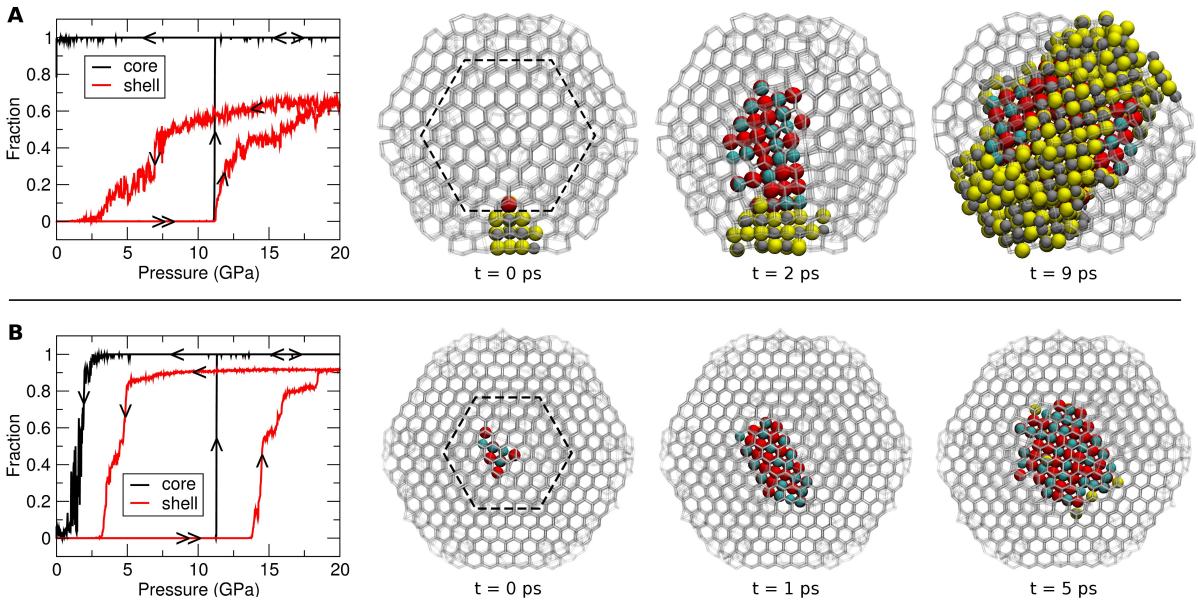


FIG. 3. **The nucleation mechanism changes with increasing shell thickness.** (**A**) (Left) Fraction of 6-coordinated atoms as a function of pressure in the core (black) and shell (red) of a 1.2 nm shell crystal. The transformation of both core and shell start around 11 GPa. (Right) Cross sections highlight stages of the nucleation process, as seen along the wurtzite c-axis. The dashed line marks the interface between core and shell. Atoms that have undergone a change of coordination are shown opaque. (For clarity, only clusters of 10 atoms or more are shown.) The transformation nucleates at the crystal surface and propagates inward. (**B**) (Left) Fraction of 6-coordinated atoms of a 2 nm shell crystal. The transformations of the core and shell happen at different pressures, around 11 and 14 GPa, respectively. (Right) Snapshots show that the nucleus is located in the core.

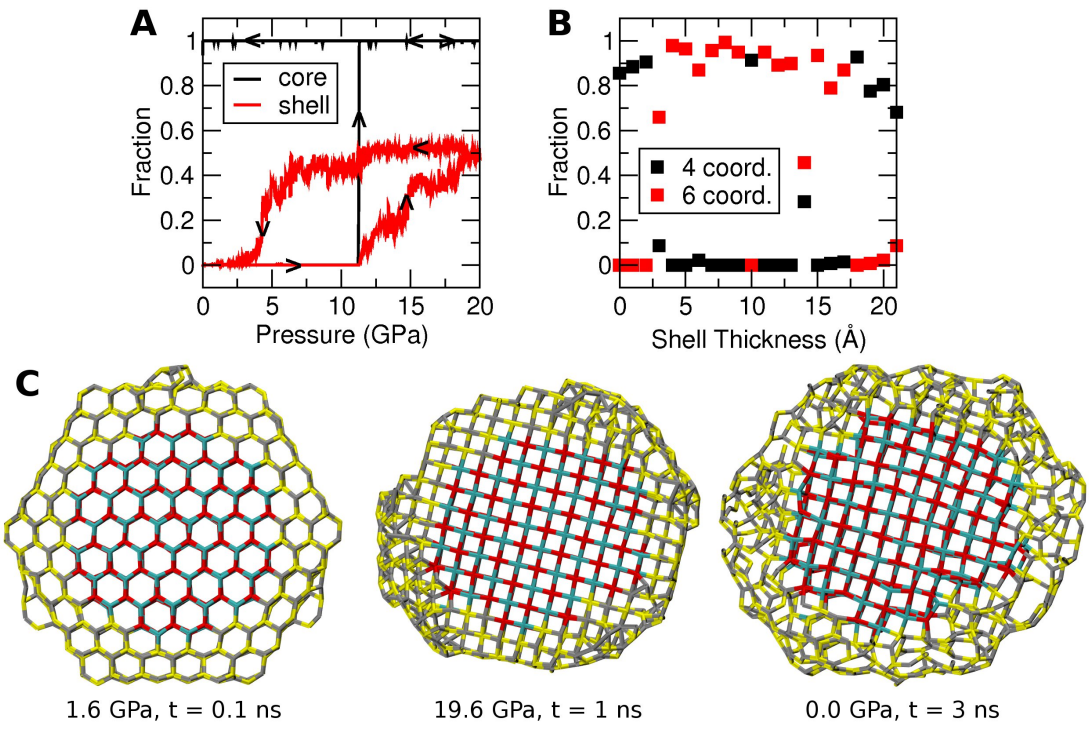


FIG. 4. **Rocksalt metastability at ambient pressure.** (**A**) Fraction of 6-coordinated atoms in the core (black) and shell (red) of a 0.9 nm shell crystal as the pressure is increased to 20 GPa and then released again. The rocksalt to wurtzite transformation at around 11 GPa is well visible. While the shell undergoes the back-transformation at around 5 GPa, the core remains in the rocksalt structure even at zero pressure. (**B**) Fraction of 4- and 6-coordinated atoms in the core, 1 ns after completing the pressure cycle. While crystals with very thin (< 0.4 nm) and thick (> 1.7 nm) shells transform back, crystals in a range of intermediate shell thicknesses remain in the rocksalt structure. (**C**) Cross sections of a 0.9 nm shell crystal at different points in the pressure cycle, viewed along the wurtzite c-axis. (Left) At an up-stroke pressure of 1.6 GPa, both core and shell are in the wurtzite structure. (Middle) At 19.6 GPa the crystal is in the rocksalt structure. (Right) A nanosecond after completing the pressure cycle, the rocksalt structure in the core persists. The shell has transformed back into a predominantly amorphous 4-coordinated structure.

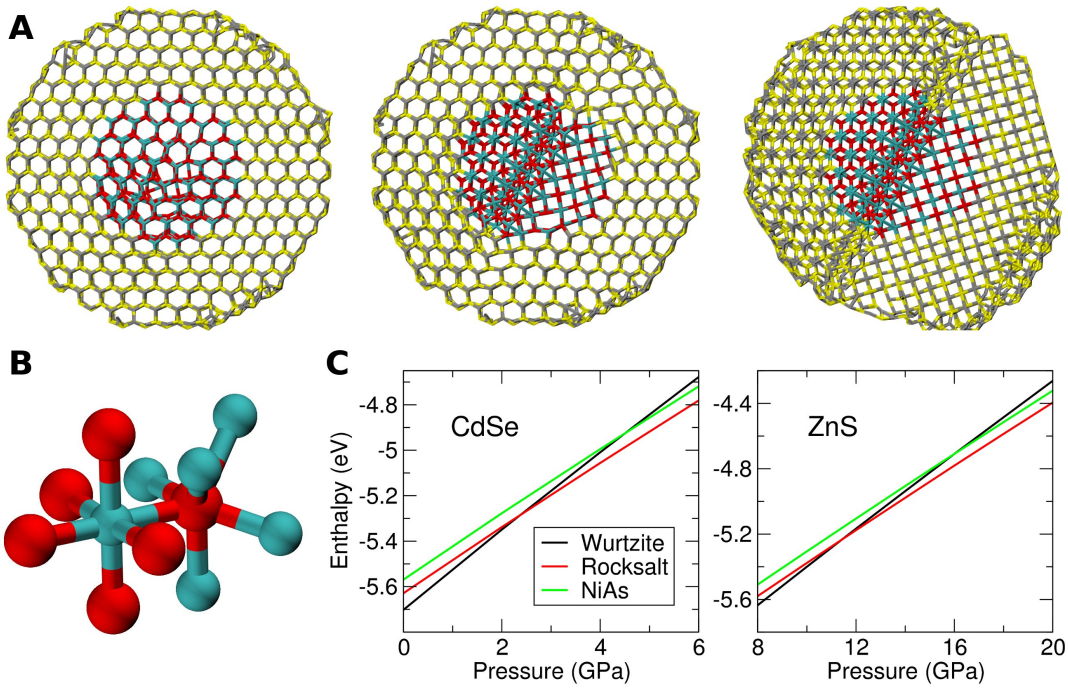


FIG. 5. **NiAs structure nucleates at high pressures.** (**A**) Time series of cross-sections of a 1.9 nm-shell nanocrystal undergoing transforming from wurtzite to NiAs/rocksalt. The crystal is viewed along the wurtzite c-axis and the same set of atoms is displayed throughout. (Left) First stage of nucleation in the core at 17 GPa. (Center) 4 ps later, no 4-coordinated atoms remain in the core and a grain boundary between NiAs (upper left part of the crystal) and rocksalt (lower right part) is visible. The shell is visibly strained, but still wurtzite. (Right) At 20 GPa, no four-coordinated atoms remain; the NiAs grain-boundary spans the entire crystal. (**B**) Close-up view of a patch of CdSe in the NiAs structure, highlighting the different coordination environments of Cd (blue) and Se (red) atoms. (**C**) Bulk enthalpies per atom as a function of pressure for CdSe and ZnS in the wurtzite, rocksalt and NiAs structures. Throughout the pressure range studied (0–20 GPa), NiAs is never stable. It is metastable with respect to the wurtzite structure at pressures larger than 4.5 GPa and 16 GPa, for CdSe and ZnS, respectively.